Classification of Deforestation Factors in 6G Satellite Forest Images

Yuhai Li[1(✉)], Yuxin Sun[1(✉)], Xianglong Meng[2], and Liang Xi[2]

[1] Science and Technology on Electro-Optical Information Security Control Laboratory, Tianjin 300300, China
liyuhai.cn@qq.com, sunyuxin@tju.edu.cn

[2] School of Computer Science and Technology, Harbin University of Science and Technology, Harbin 150080, China

Abstract. The terrestrial satellite network will play an essential role in 6G. Through the satellite system, people can obtain a lot of ground image information to process tasks and feedback. Forest resource is an essential resource. Determining the causes of deforestation is crucial for the development and implementation of forest protection plans. In this article, we propose a novel deep neural network model for distinguishing drivers of deforestation events from satellite forest images. To solve the problems of image rotation caused by satellite angle rotation and image blurring caused by extreme weather occlusion during satellite image acquisition, we add data enhancement and a self-supervised rotation loss to the model to improve the robustness and adaptability. We use deforestation maps generated from Landsat 8 satellite imagery as a dataset and demonstrate that our approach achieves better results than the baselines.

Keywords: 6G network · deforestation factor classification · deep learning

1 Introduction

Radio communication technology has developed rapidly. The fifth-generation mobile information system (5G) is combined with the Internet of things. Radio communication technology can meet more and more application needs, and communication speed is getting faster and faster. Now, we has begun to move towards the sixth generation mobile information system (6G).

On the basis of 5G technologies, The 6G network will be fully connected communication network with global coverage, combining terrestrial communication network and space satellite communication network. So, in 6G, terrestrial-satellite networks (TSN) will become the critical leverage to explore airspace resources for communications [1]. Through the integration of satellite signals, global seamless signal coverage, the global positioning satellite system, image satellite system and 6G ground network, the 6G network can help people quickly explore the ground information.

In modern times, protecting forest resources can prevent species extinction, create clean air and water, and detect climate change [2]. For some reason, forest loss in the

A. Li et al. (Eds.): 6GN 2022, LNICST 504, pp. 196–207, 2023.
https://doi.org/10.1007/978-3-031-36011-4_17

tropics results in about 10% of the world's annual greenhouse gas emissions [3], which should be reduced to decrease the potential for climate tipping points [4]. The direct factors or specific activities leading to the deforestation of tropical rainforests include natural events (such as fire and flood), manufactured land occupation (such as industrial and agricultural development), and human activities [5]. Accurately identifying these factors is crucial for implementing targeted policies and actions to protect forests. In terms of the rate of rainforest loss, Indonesia ranks among the highest in the world, so analyzing the causes of forest loss in Indonesia can help us to classify forest loss factors globally.

Through the 6G ground-satellite network interconnection system, we can obtain high-resolution forest satellite images to analyze the direct causes of forest loss and provide essential information for conservation work. With the development of interconnectivity between satellites and terrestrial networks, and the advances in various deep learning methods, it possible to obtain and analyze terrestrial geographic information automatically. Compared with the previous machine learning methods, such as decision trees, random forest classifiers, etc. [6–9], Convolutional neural network (CNN) is the most effective method for extracting data features [10–13]. However, these CNN-based methods usually only use clear and standard data for model training, the performance becomes unstable once the data changes, such as image angle changes due to satellite rotation or image blurring due to cloud or fog interference.

In this paper, considering the increasing the data diversity, we present a new model based on the CNN network to classify deforestation images. We used an encoder, a classification header, and an angle prediction header. Through data fuzzy and rotation processing, the model can by trained more deeply by the combined data and predict the factors of forest loss more efficiently and accurately. We used the satellite forest image dataset of Indonesia processed and made by Irvin et al. [14] to conduct the experiments. The results show that our model has high robustness and classification accuracy.

2 Related Work

2.1 6G Network

In the era of the 5G networks, it is expected that more than 80% of land areas and more than 95% of sea areas could not be covered by satellite signals. Moreover, as the signal range of the 5G network is concentrated within 10km above the ground, the actual "global Omni-sphere" and "Internet of Things' cannot be truly realized. To this end, 6G will be further upgraded based on 5G, featuring complete coverage and application.

For the global signal coverage, 6G satellite communication will play an important role. By integrating the satellite networks with the ground networks, 6G can achieve the goal of global mobile network coverage, and People all over the world can use it anytime, anywhere.

6G satellite network has been able to provide complementary satellite services in many areas, and satellite services have evolved from traditional voice and broadcast services to broadband Internet services [15]. It can detect the movements of ground users, ground information, vehicles, emergency base stations, and other satellites [16], and predict weather conditions. By transmitting detected statistics or captured satellite images to the ground, combined with models trained through artificial intelligence technology, it can effectively respond to current geographic information or weather disasters.

Therefore, we use the 6G satellite image dataset of Indonesia's rainforests to analysis why they are being cut down. The used 6G ground-space satellite network framework is shown in Fig. 1.

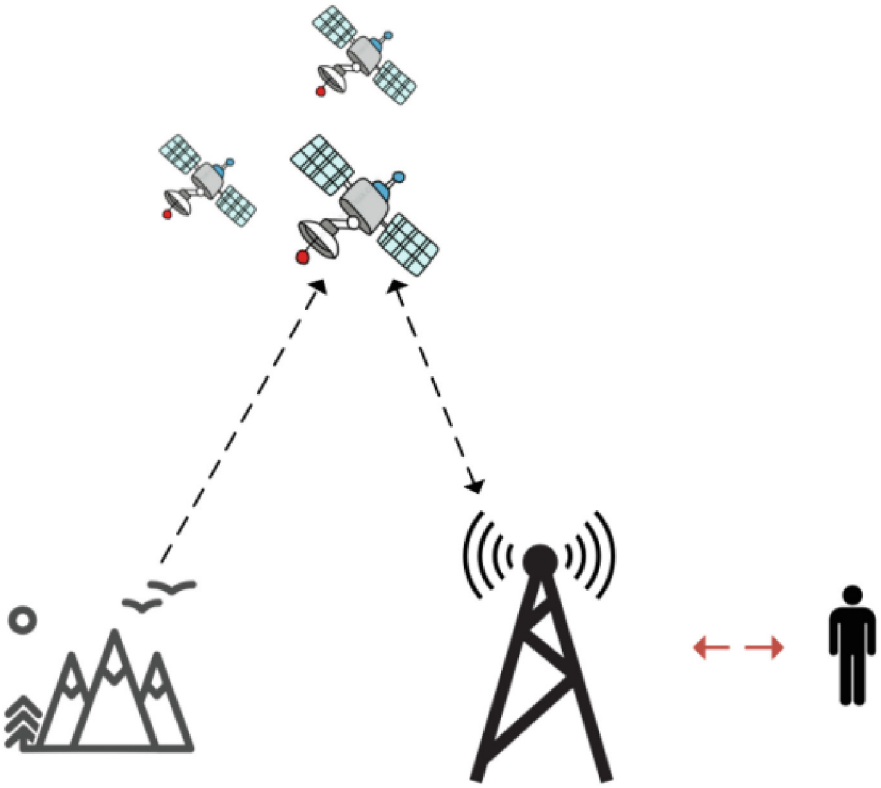

Fig. 1. 6G ground-space satellite network

2.2 Resnet Network

With the increase of layers of neural networks, the problem of vanishing/exploding gradients would appear [17, 18]. In the early, this problem was solved to some extent by

normalized initialization [18–20], which used stochastic gradient descent and backpropagation [21], but it also exposed another problem: as the number of layers of the neural network increases, the network accuracy peaks and then drops off at a high-speed rate.

In view of the above problems, Kaiming He [22] proposes the Resnet network framework. Resnet network is mainly composed of two/three-layer residual blocks. In the [22], five network frameworks are proposed: 18-layer, 34-layer, 50-layer, 101-layer, and 152-layer. The network framework of Resnet18 is adopted in this paper, and its framework parameters are shown in Table 1. From the parameter table, we can know the image information is constantly changing through each network layer. The network framework is shown in Fig. 2. There are four residual blocks are used in Resnet18, each consisting of two basic blocks, the details are shown in Fig. 3. In Resnet18, each basic block is a double-layer foundation block consisting of two convolutions and a short circuit connection. Figure 4 shows the detailed structure of the basic block.

Because Resnet18 network framework has the advantages of no gradient disappearance/gradient explosion and network degradation compared with the convolutional network, we choose it as our encoder to extract image features.

Table 1. Resnet18 Network framework

Layer name	Output size	18-layer
Conv1	112 × 112	7 × 7, 64, stride 2
Residual block_1	56 × 56	3 × 3 max pool, stride 2
		$\begin{bmatrix} 3 \times 3 & 64 \\ 3 \times 3 & 64 \end{bmatrix} \times 2$
Residual block_2	28 × 28	$\begin{bmatrix} 3 \times 3 & 128 \\ 3 \times 3 & 128 \end{bmatrix} \times 2$
Residual block_3	14 × 14	$\begin{bmatrix} 3 \times 3 & 256 \\ 3 \times 3 & 256 \end{bmatrix} \times 2$
Residual block_4	7 × 7	$\begin{bmatrix} 3 \times 3 & 512 \\ 3 \times 3 & 512 \end{bmatrix} \times 2$
	1 × 1	Average pool, 512-d fc, SoftMax
FLOPs		1.8×10^9

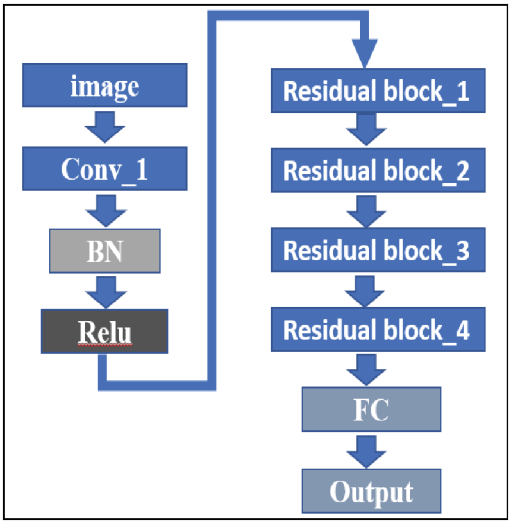

Fig. 2. Resnet18 network model

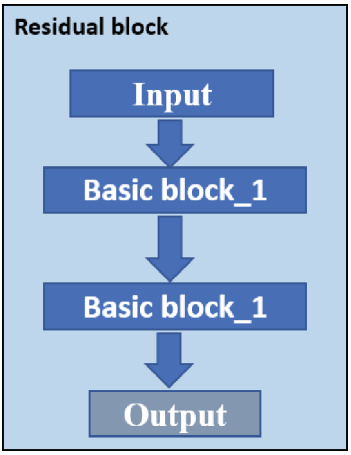

Fig. 3. Residual block

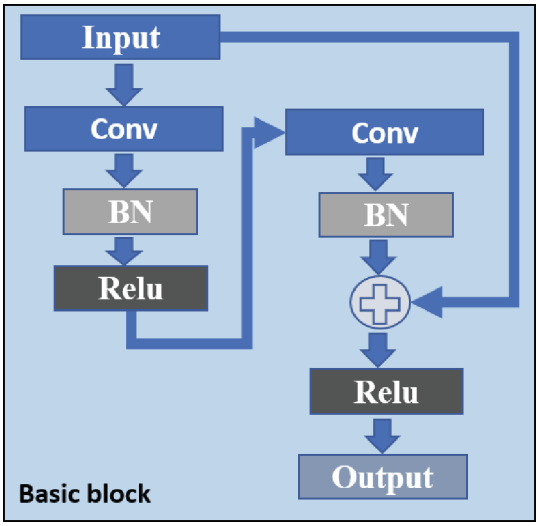

Fig. 4. Basic block of Resnet18

3 Method

We change the image size from 332 × 332 to 160 × 160. The input data are defined as $x = \{(x_i, y_i)\}_{i=1}^{N}$, Where N is the number of data. $y_i \in \{1 \ldots\ldots C\}$ is the labels of x_i, C represents the number of classes. This method carries out fuzzy and rotation processing on the original data, x, and get the processed sample, defined as $x^g = \{(x_i^g)\}_{i=1}^{N}$ and $x^r = \{(x_i^r, y_i^r)\}_{i=1}^{N}$, where x^g represents the data of x after rotation and fuzzy enhancement. x^r

represents the data augmented by rotation only, and the rotation label, $y_i^r \in \{0, 1, 2, 3\}$ is generated by its rotation angle, respectively representing rotation 0^o, 90^o, 180^o, 270^o (Fig. 5).

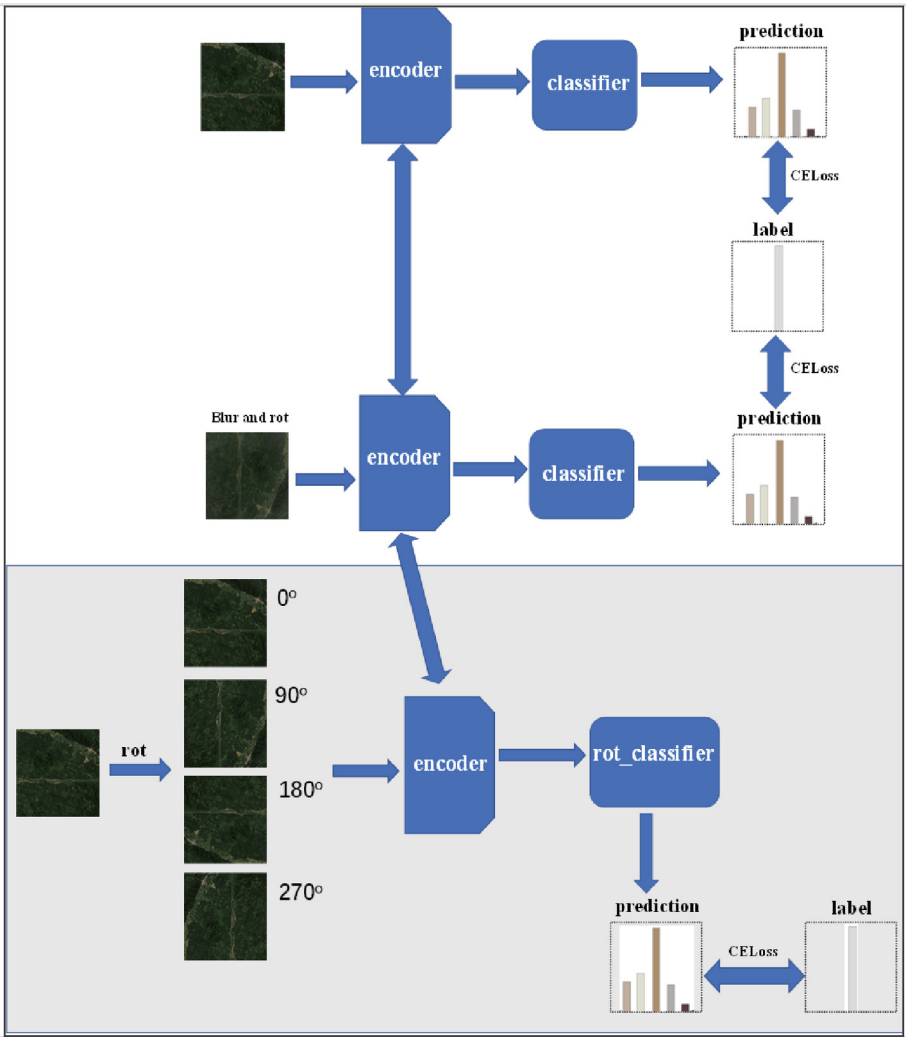

Fig. 5. Model framework: The standard supervised learning module is shown on the white background, and the rotating self-supervised learning model is shown on the gray background.

Our model defines the encoder as $E: X \rightarrow F$, where F is the extracted picture feature vector. Then we represent a rotation Angle predictor f_r: $F \rightarrow p^r$ and a classifier f_c: $F \rightarrow p^c$ for data classification and rotation Angle prediction. The details are mainly in five parts.

(1) Our encoder structure uses the model framework of Resnet18 proposed by Kaiming He et al. [11]. It consists of 17 convolutional layers and one fully connected layer.

(2) The classifier and the rotation angle predictor use three linear layers to reduce the dimension of the features extracted by the encoder and finally output the classification and angle prediction.

(3) We use encoders and predictors with the same framework as classification prediction and share the weight of the encoder.

(4) Moreover, by data enhancement with fuzzy and rotation, the model can avoid unclear satellite images caused by extreme weather, such as fog, typhoons, and shape changes of areas due to satellite rotation, which can lead to the inaccurate identification of deforestation factors.

We use the cross-entropy to calculate the loss of our encoder and classifier, and our actual loss function is shown below:

$$L_c = \frac{1}{2B} \sum_{b=1}^{2B} H(y_b, p(y|x_b)) \tag{1}$$

where B represents the size of batch size, x_b represents the labeled data, x and x^g, $p(y|x_b) = softmax(f(E(x_b)))$ is classification prediction. H is the cross-entropy between y_b and $p(y|x_b)$.

(5) For the prediction of rotation angle, we randomly rotate the original image to generate forest images from different angles, so that the model can learn the rotated image separately. By comparing with the original image, the rotation angle of the image can be derived successfully, which improves the robustness and identification ability of the model.

We use the cross-entropy to calculate the loss of our encoder-predictor, and the formula is as follows:

$$L_r = \frac{1}{B} \sum_{b=1}^{B} H(y_b^r, p(y^r|x_b^r)) \tag{2}$$

where x_b^r represents the rotation data in x^r, $p(y^r|x_b^r) = softmax(f\left(E\left(x_b^r\right)\right))$ is the output of the predictor.

In short, the final loss function is as follows:

$$Loss = L_r + L_c \tag{3}$$

L_r is the rotation loss, and L_c is the supervision loss.

The details of our model are shown in Algorithm 1.

Algorithm 1 Forest loss classification

Input: Labeled data, $x = \{(x_i, y_i)\}_{i=1}^{N}$; fuzzy data, $x^g = \{(x_i^g)\}_{i=1}^{N}$; Batch size, b; Epoch number, e

1. while e<$epoch$ do
2. for i=1 to b do
3. $x_i^r = rotate(x_i)$
4. $y_b = f_c(E(x))$
5. $y_b^g = f_c(E(x^g))$
6. $y_b^r = f_r(E(x^r))$
7. The loss is calculated by the Formula (1), (2), (3)
8. End for
9. End while

4 Experiment

4.1 The Dataset

In this work, we use the same dataset as Irvin et al. [14], where annotations on deforestation events are curated by Austin et al. [23]. These images of natural forest loss are from the global forest change (GFC) map with 30 million resolution published from 2001 to 2016. The GFC map contains satellite forest images with various types and resolutions. The missing images were classified and annotated by Austin et al. [23]. The main reasons and classifications of deforestation are shown in Table 2. Figure 6 provides some examples of each class. Table 3 shows the details of each group. We use the relationship between deforestation factors and classification factors and the partition method of training/validation/test set given by Irvin et al. [14].

Table 2. The reasons and classifications of deforestation details of the dataset.

Deforestation Category	Classification
Oil palm plantation Timber plantation Other large-scale plantations	Plantation
Grassland/shrubland	Grassland/shrubland
Small-scale agriculture Small-scale mixed plantation Small-scale oil palm plantation	Smallholder agriculture
Mining Fishpond Logging road Secondary forest Other	Other

Fig. 6. Data instances from left to right and top to bottom are Plantation, Smallholder agriculture, Grassland/shrubland, etc.

Table 3. The details of dataset according to [11].

Classification	Training	Validation	Test
Plantation	686	219	265
Grassland/shrubland	556	138	207
Smallholder agriculture	143	47	85
Other	231	70	112
Overall	1616	474	669

4.2 Experimental Settings

In this experiment, we perform the experiments on a Server with NVIDIA GeForce RTX 3090, and the framework is PyTorch. The learning rate of the model was set to 0.001, and the Adam algorithm was used to optimize the neural network. The model was trained by 300 epochs, and the batch size was set to 16.

4.3 Results and Analysis

We test the performance of our proposed model on a dataset of Indonesian deforestation factors [14] and compare it with a supervised approach that only applies the Resnet18 as an encoder. According to the results in Table 4, we can see that the performances of our model on the training set, validation set, and test set are better than that of the comparative method. Specially, on the test set, our model achieves an accuracy of 66.42%, which is 7% higher than the comparative method's 59.03%. The experimental results directly verify that our model can accurately classify deforestation data images. In addition, through experimental tests, the experimental resources occupied by the self-supervised module and the supervised learning module are almost the same, which proves the availability of our model.

Table 4. Experimental results of our model and the baseline

Model	Train	Validation	Test
Resnet18-Supervised	99.56	67.64	59.03
Resnet18-Our	99.75	72.8	66.42

5 Conclusion

We propose a new deep learning model for deforestation factor classification in 6G satellite forest images. The model's performance can not be disturbed even in the face of clouds or extreme weather. In addition, the classification prediction of the model can be stable even by applying the data rotation and self-supervised method. Compared with traditional deep learning methods, the classification accuracy of our model is improved by 7%. The results show that our approach has a more substantial effect than other methods. In the future, with the continuous development of the 6G technology, how to better connect the 6G satellite network with the model and improve the operation efficiency will be our next project.

Acknowledgments. This work was supported by Heilongjiang Province Natural Science Foundation under Grant LH2022F034.

References

1. Fu, S., Gao, J., Zhao, L.: Integrated resource management for terrestrial-satellite systems. IEEE Trans. Veh. Technol. **69**(3), 3256–3266 (2020)
2. Foley, J.A., et al.: Global consequences of land use. Science **309**(5734), 570–574 (2005)
3. Arneth, A., et al.: "Ipcc special report on climate change". Desertification, Land Degradation, Sustainable Land Management, Food Security, and Greenhouse Gas Fluxes in Terrestrial Ecosystems (2019)
4. Lenton, T.M., et al.: Climate tipping points — too risky to bet against. Nature **575**(7784), 592–595 (2019). https://doi.org/10.1038/d41586-019-03595-0
5. Hosonuma, N., et al.: An assessment of deforestation and forest degradation drivers in developing countries. Environ. Res. Lett. **7**(4), 044009 (2012)
6. Phiri, D., Morgenroth, J., Cong, X.: Long-Term land cover change in Zambia: an assessment of driving factors. Sci. Total Environ. **697**, 134206 (2019)
7. Descals, A., Szantoi, Z., Meijaard, E., Sutikno, H., Rindanata, G., Wich, S.: Oil palm (Elaeis Guineensis) mapping with details: smallholder versus industrial plantations and their extent in Riau, Sumatra. Remote Sens. **11**(21), 2590 (2019)
8. Poortinga, A., et al.: Mapping plantations in Myanmar by fusing landsat-8, sentinel-2 and sentinel-1 data along with systematic error quantification. Remote Sens. **11**(7), 831 (2019)
9. Hethcoat, M.G., Edwards, D.P., Carreiras, J.M.B., Bryant, R.G., França, F.M., Quegan, S.: A machine learning approach to map tropical selective logging. Remote Sens. Environ. **221**, 569–582 (2019)
10. Sohn, K., Berthelot, D., Carlini, N., et al.: Fixmatch: simplifying semi-supervised learning with consistency and confidence. Adv. Neural. Inf. Process. Syst. **33**, 596–608 (2020)
11. Berthelot, D., Carlini, N., Cubuk, E.D., et al.: ReMixMatch: semi-supervised learning with distribution alignment and augmentation anchoring. arXiv preprint arXiv:1911.09785 (2019)
12. Hu, Z., Yang, Z., Hu, X., Nevatia, R.: SimPLE: similar pseudo label exploitation for semisupervised classification. In: Proceedings of the IEEE/CVF Conference on Computer Vision and Pattern Recognition, pp. 15099–15108. IEEE, Nashville (2021)
13. Mitton, J., Murray-Smith, R.: Rotation Equivariant deforestation segmentation and driver classification. arXiv preprint arXiv:2110.13097 (2021)
14. Irvin, J., Sheng, H., Ramachandran, N., Johnson-Yu, S., Zhou, S., Story, K., et al.: ForestNet: classifying drivers of deforestation in Indonesia using deep learning on satellite imagery. arXiv preprint arXiv:2011.05479 (2020)
15. Botta, A., Pescape, A.: On the performance of new generation satellite broadband Internet services. IEEE Commun. Mag. **52**(6), 202–209 (2014)
16. Chini, P., Giambene, G., Kota, S.: A survey on mobile satellite systems. Int. J. Sat. Commun. **28**(1), 29–57 (2010)
17. Bengio, Y., Simard, P., Frasconi, P.: Learning long-term dependencies with gradient descent is difficult. IEEE Trans. Neural Networks **5**(2), 157–166 (1994)
18. Glorot, X., Bengio, Y.: Understanding the difficulty of training deep feedforward neural networks. In: AISTATS (2010)
19. LeCun, Y., Bottou, L., Orr, G.B., Müller, K.-R.: Efficient backprop. In: Orr, G.B., Müller, K.-R. (eds.) Neural Networks: Tricks of the Trade. Lecture Notes in Computer Science, vol. 1524, pp. 9–50. Springer, Heidelberg (1998). https://doi.org/10.1007/3-540-49430-8_2
20. He, K., Zhang, X., Ren, S., Sun, J.: Delving deep into rectifiers: surpassing human-level performance on ImageNet classification. In: ICCV (2015)
21. LeCun, Y., et al.: Backpropagation applied to handwritten zip code recognition. Neural Comput. **1**(4), 541–551 (1989)

22. He, K., Zhang, X., Ren, S., Sun, J.: Deep residual learning for image recognition. In: Proceedings of the IEEE Conference on Computer Vision and Pattern Recognition, pp. 770–778. IEEE, Las Vegas (2016)
23. Austin, K.G., Schwantes, A., Yaofeng, G., Kasibhatla, P.S.: What causes deforestation in Indonesia? Environ. Res. Lett. **14**(2), 024007 (2019)